

## Diffusion mechanisms and the nature of Si ad-dimers on Ge(001)

E. Zoethout, H. J. W. Zandvliet, W. Wulfhchel, Georg Rosenfeld, and Bene Poelsema

*Department of Applied Physics and Centre of Materials Research, University of Twente, P.O. Box 217, 7500 AE Enschede, The Netherlands*

(Received 18 June 1998)

The thermal motion of Si ad-dimers on Ge(001) has been studied with scanning tunneling microscopy. At room temperature the Si ad-dimers residing on top of the substrate dimer rows perform a one-dimensional random walk along the substrate dimer rows. The activation barrier for the diffusion process is estimated to be 0.83 eV. Although the preferential diffusion direction is along the substrate dimer rows, also diffusion across the rows has been observed. The latter diffusion process consists of two separate events: a jump of a Si ad-dimer from an on-top position to a position in the trough between the substrate dimer rows and a hop from a trough position to an on-top position. [S0163-1829(98)02448-5]

With the advent of the scanning tunneling microscope (STM), it has become possible to study important surface processes, such as surface diffusion and thermal step fluctuations, in real space with atomic resolution. Despite extensive experimental and theoretical studies, many fundamental questions remain open even about relatively simple processes. In this paper, we will focus on the dynamics of Si ad-dimers on the Ge(001) surface. The Si on Ge(001) system has been studied in less detail than the systems Si on Si(001) and Ge on Si(001). This is remarkable because knowledge about the kinetic processes during growth of Ge on Si as well as Si on Ge are of equal importance for understanding the epitaxial growth of the technologically important Si/Ge heterostructures. Recently, however, we have studied the dynamics and energetics of this system at room temperature.<sup>1</sup> Various dynamic events, such as diffusion of Si ad-dimers along and across substrate dimer rows, have been observed. Here, we present a more detailed analysis of those dynamic events including the determination of their activation energies.

The experiments are performed in an ultrahigh-vacuum system equipped with a scanning tunneling microscope. The nominally flat *n*-type Ge(001) samples are nearly intrinsic (34–60  $\Omega$  cm). Crystal cleaning involves resistive heating to 800 K for 24 h, followed by several cycles of 800 eV Ar<sup>+</sup> ion bombardment and subsequent annealing at 1100 K. The samples are either radiation quenched or slowly cooled (1 K/s) to room temperature. Samples cleaned in this way typically contain 0.02–0.5 % surface defects. Si was deposited from a resistively heated crystal while the Ge substrate was kept at room temperature. After the deposition, the samples were transferred *in situ* to the STM for imaging.

We have analyzed a large number of STM images taken after room-temperature deposition of a few percent of a monolayer of Si and have found no evidence for the existence of Si monomers. The smallest observed features turn out to be Si ad-dimers. Conventional wisdom among Si/Ge crystal growers holds that a thermal silicon source produces only atoms. Analysis of a thermal silicon source similar to the one used here by Honig<sup>2</sup> demonstrated an output of nearly 100% Si atoms. The observation of Si ad-dimers and even larger clusters of Si atoms after room temperature depo-

sition of only a few percent of a monolayer Si on Ge(001) suggests that Si atoms must be very mobile at room temperature. In Fig. 1 a schematic diagram of the various adsorption sites for a Si ad-dimer and a Si monomer is shown. In order to compare our results with the model system Si/Si(001), we first briefly summarize the dynamics of Si on Si(001). A low-temperature STM study<sup>3</sup> has revealed that isolated Si adatoms on Si(001) are located at nonepitaxial sites and are even mobile at temperatures as low as 160 K. After a deposition of 0.02 monolayers of Si, roughly half of the deposited adatoms at 160 K eventually form ad-dimers situated on top of the substrate dimer rows. At room temperature adatoms quickly form ad-dimers, but these are then hindered to form larger structures due to the large barrier for ad-dimer diffusion. At temperatures near and above room temperature, diffusion and rotation of Si ad-dimers on Si(001) have been studied in detail by several groups.<sup>3–9</sup> The first study of the diffusion of ad-dimers on Si(001) was reported by Dijkamp, van Loenen, and Elswijk.<sup>4</sup> These authors showed that ad-dimers situated on top of the substrate dimer rows diffuse preferentially along the dimer rows with a diffusion barrier of  $1 \pm 0.1$  eV and an attempt frequency of  $10^{13}$  Hz. A few years later, Swartzentruber<sup>6</sup> used the atom-tracking technique to directly follow the diffusion of ad-dimers. From the hopping rates measured at various temperatures, he extracted a diffusion barrier of  $0.94 \pm 0.09$  eV and a prefactor of  $10^{12.8 \pm 1.3}$  Hz. Recently, a rotational transition of a Si ad-dimers located on top of the substrate dimer rows of Si(001) was found to occur at room temperature on a time scale of seconds.<sup>5,7</sup> Two configurations for a Si ad-dimer situated on

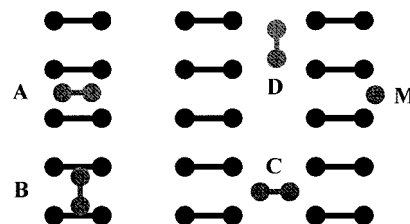


FIG. 1. Schematic diagram of the various adsorption sites for Si ad-dimers. Black dumbbells: Ge dimers; gray dumbbells: adsorbed Si dimers; gray atom: adsorbed Si adatom.

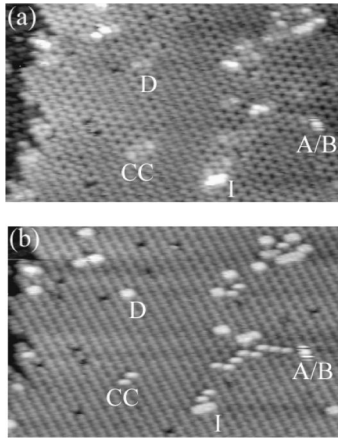


FIG. 2. Scanning tunneling microscopy image of Ge(001) after deposition of 0.01 monolayer Si at room temperature. Structures  $A/B$  and  $D$  refer to various adsorption sites for Si ad-dimers.  $I$  refers to epitaxial islands consisting of an array of  $D$  and  $B$  ad-dimers.  $CC$  structures consist of  $C$  features which are aligned along  $\langle 130 \rangle$  directions. (a) Filled-state image. Sample bias  $-1.6$  V, tunneling current  $1$  nA, and image size  $380 \text{ \AA} \times 220 \text{ \AA}$ . (b) Empty-state image. Sample bias  $+1.6$  V, tunneling current  $1$  nA, and image size  $380 \text{ \AA} \times 220 \text{ \AA}$ .

top of the substrate dimer rows, denoted  $A$  and  $B$ , respectively, are identified.<sup>5</sup> The  $A$  ( $B$ ) state has its dimer bond aligned parallel (perpendicular) to the substrate dimer bonds. The rotational barrier for the  $B$  to  $A$  ( $A$  to  $B$ ) state was measured to be  $0.74 \pm 0.01$  eV ( $0.68 \pm 0.01$  eV).<sup>7</sup> Finally, Borovsky, Krueger, and Ganz<sup>8</sup> have reported a diffusion pathway for Si ad-dimers across substrate dimer rows of Si(001). They showed that at a temperature of  $450$  K the Si ad-dimer situated at an on-top site occasionally hops to a position in between the substrate dimer rows, i.e., a trough position. The activation barrier for the cross channel diffusion was measured to be  $1.36 \pm 0.06$  eV. Moreover, these authors argued that a dissociation process of the Si ad-dimer cannot be responsible for the ad-dimer diffusion across the substrate dimer rows.

In filled- and empty-state STM images (see Fig. 2), various types of Si ad-clusters—small features on top of substrate dimer rows ( $B, A/B$ ), small features between dimer rows ( $D$ ), and larger features extending over several dimer rows ( $CC, I$ )—can be identified. The  $I$  structures are aligned perpendicular to the substrate dimer rows and consist of an array of dimers in  $BD$  registry. The  $CC$  structures are aligned along  $\langle 130 \rangle$  directions and consist of features (ad-dimers<sup>1</sup> or atom paired units<sup>10</sup>) that are positioned in the trough between the substrate rows. Small features residing on top of the substrate dimer rows can be divided into two categories: immobile ad-dimers which are attached to surface defects or impurities and mobile ad-dimers which are denoted  $A/B$  ad-dimers. Two stable configurations for the Si ad-dimer residing on top of a dimer row of Si(001) were predicted by Brocks, Kelly, and Car,<sup>11</sup> who carried out *ab initio* calculations. They found a preference for state  $A$ , where the ad-dimer bond is aligned along the substrate dimer bond. Zhang *et al.*<sup>5</sup> carried out calculations using the empirical Stillinger-Weber potential and found that state  $B$ , where the ad-dimer bond is aligned perpendicular to the substrate

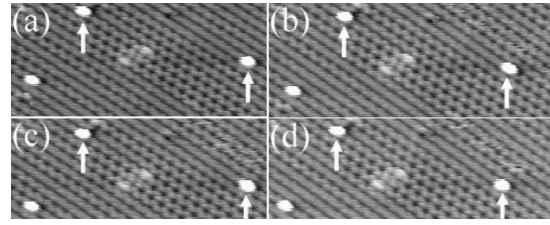


FIG. 3. Four subsequent filled-state STM images of pinned Si ad-dimers. Image size  $210 \text{ \AA} \times 80 \text{ \AA}$ . Sample bias  $-1.6$  V and tunneling current  $0.4$  nA.

dimer bond, has a lower energy. Room-temperature STM experiments<sup>3,12</sup> revealed that both states do occur at room temperature with a distinct preference for state  $B$ . From the relative occupations of both states, an energy difference of  $60 \pm 10$  meV was found.<sup>5,7</sup> Moreover, a rotational transition from state  $A$  to state  $B$  and vice versa was found to occur on a time scale of seconds at room temperature.<sup>5,7,12</sup> For Si ad-dimers residing at on-top positions of Ge(001) substrate dimer rows, the situation turns out to be somewhat different. Quite frequently, Si ad-dimers attached to surface defects such as missing dimer defects are found. The majority of these Si ad-dimers are found in configuration  $B$  and are immobile (Fig. 3). The on-top Si ad-dimers that are not attached to surface defects are mobile at room temperature and exhibit a frizzy round appearance. Because this frizzy round appearance makes it impossible for us to discriminate between an ad-dimer in state  $A$  and state  $B$ , we label these ad-dimers as  $A/B$  dimers (Fig. 4). The  $A/B$  dimers are deforming during the relatively short period of time that they are scanned by the tip, resulting in a frizzy appearance (a statistical analysis of several films and knowledge of the diffusion barrier for  $A/B$  dimers along the substrate dimer rows reveals that the changes of the  $A/B$  dimer can hardly be due to thermal motion or displacement by the tip along the substrate dimer rows). The field of the tip appears not to be a dominant factor here, as changing the field strength and more or less frequent scanning over the same dimer does not change the results significantly. On the average, there are typically two to three changes of the  $A/B$  features during scanning of the  $A/B$  feature (typically  $100$  ms), resulting in an activation energy of the rate limiting step of  $0.7$  eV (assuming a prefactor of  $10^{13}$  Hz).

Besides the rotational mode of Si ad-dimers in on-top positions, these mobile dimers also perform a random walk along the substrate dimer rows. Yamasaki, Uda, and Terakura<sup>13</sup> found an upper bound of the activation energy of  $1.45$  eV for diffusion of a Si ad-dimer along the top of a Si(001) substrate dimer row. [Goringe and Bowler<sup>14</sup> studied theoretically the trough diffusion of a Si ad-dimer on Si(001).] In Fig. 5, the diffusion of an on-top dimer ( $A/B$ ) along the substrate dimer row is displayed. In Fig. 5, a  $D$  dimer first diffuses in the trough before it jumps to an on-top position [Fig. 5(c)]. At the on-top position the ad-dimer diffuses rapidly along the substrate dimer row. Since many Si ad-dimers situated at on-top sites are immobile because they are attached to surface defects, we have ignored these immobile ad-dimers in the determination of the diffusion barrier. In Fig. 6, the mean-square displacement versus time of a mobile  $A/B$  ad-dimer is displayed. The diffusing ad-dimer is

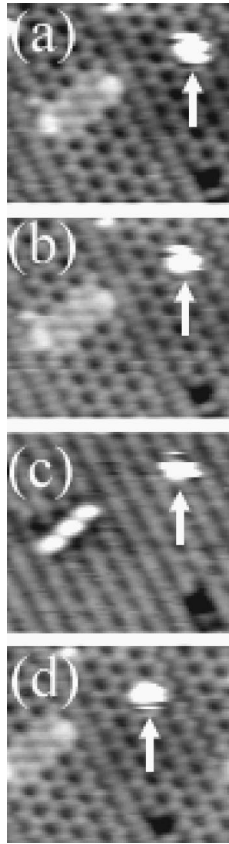


FIG. 4. Four subsequent STM images (image size  $70 \text{ \AA} \times 75 \text{ \AA}$ ). Time lapse between the images is 150 s. (a), (b), and (d) Sample bias  $-1.6 \text{ V}$  and tunneling current  $0.4 \text{ nA}$ . (c) Sample bias  $+1.6 \text{ V}$  and tunneling current  $0.4 \text{ nA}$ .

trapped between two surface defects and therefore performs a restricted random walk. The mean-square displacement of an unrestricted one-dimensional random walker scales linearly with time,

$$\langle x^2 \rangle = 2Dt, \quad (1)$$

where  $D = \frac{1}{2}a^2\nu$  and  $a (=4 \text{ \AA})$  is the spacing between neighboring lattice sites. It must be noted that on the small line segments available here an ad-dimer cannot perform an unrestricted one-dimensional random walk. Sooner or later the ad-dimer will collide with one of the surface defects. Unlike the mean-square displacement of an ad-dimer in an unrestricted random walk, the mean-square displacement on a finite line segment is dependent upon the point at which the ad-dimer starts its random walk. This complication can be addressed by averaging the displacements over all possible starting positions of the line segment under study. This has been done for a one-dimensional random walk obeying a Gaussian distribution along a line of length  $L$ .<sup>15</sup> For a reflecting boundary the mean-square displacement, averaged over all initial positions, can be approximated by<sup>15</sup>

$$\langle \langle x^2 \rangle \rangle \approx 2Dt \left( 1 - \frac{4}{3L} \sqrt{\frac{4Dt}{\pi}} \right). \quad (2)$$

For infinitely long line segments the original formula for unrestricted random walk is recovered. The rate of the diffusion process of the ad-dimer,  $\nu = \nu_0 \exp(-E/kT)$ , is 0.10

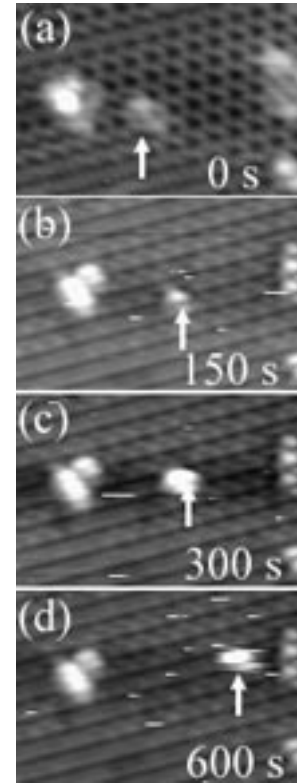


FIG. 5. Four subsequent STM images of a diffusing Si ad-dimer. Image size  $160 \text{ \AA} \times 80 \text{ \AA}$ . (a) Sample bias  $-1.6 \text{ V}$  and tunneling current  $0.4 \text{ nA}$ . (b)–(d) Sample bias  $+1.6 \text{ V}$  and tunneling current  $0.4 \text{ nA}$ . The Si ad-dimer in the  $D$  state [images (a) and (b)] converts to an  $A/B$  ad-dimer [images (c) and (d)].

$\pm 0.01 \text{ Hz}$  at room temperature, which translates into a diffusion barrier,  $E$ , of  $0.83 \pm 0.05 \text{ eV}$  assuming an attempt frequency,  $\nu_0$ , of  $10^{13 \pm 1} \text{ Hz}$ .<sup>16</sup>

Let us now discuss the structures lying in between substrate dimer rows. The only small and isolated feature positioned in the trough can be identified as a  $D$  dimer (see Fig. 7). Annealing at  $350 \text{ K}$  for five minutes results in a significant increase in the number of dimers having the  $D$  orientation while the amount of dimers in all the other configurations is reduced.<sup>1</sup> This indicates that this structure is the most stable Si ad-dimer on  $\text{Ge}(001)$ . Recently, Qin and Lagally<sup>10</sup> have shown that Ge atoms adsorbed on the  $\text{Si}(100)$  surface near room temperature form chainlike structures that consist

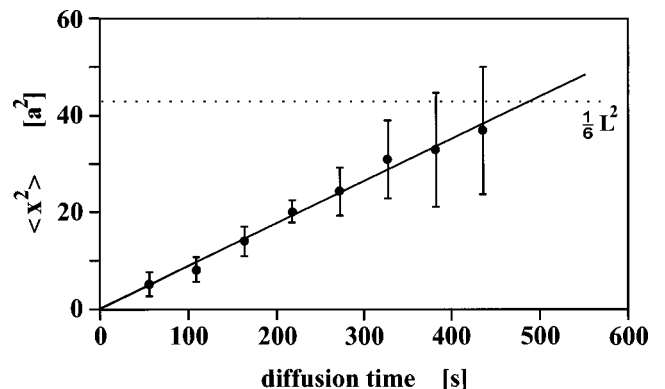


FIG. 6. Mean-square displacement,  $\langle x^2 \rangle$ , in units of  $a^2$  ( $a = 4 \text{ \AA}$ ) of a Si on-top ad-dimer versus time ( $L = 16a$ ). Eventually the mean-square displacement will saturate at  $\frac{1}{6}L^2$ .

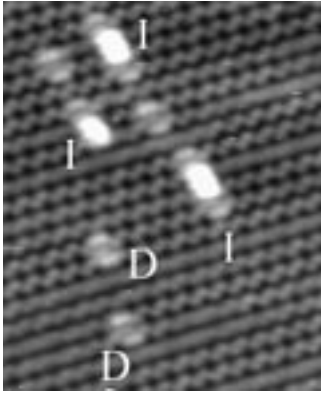


FIG. 7. High-resolution filled- ( $-1.6$  V) state STM image of 0.01 monolayer Si deposited on Ge(001). Structures  $I$  and  $D$  indicate epitaxial islands and  $D$  dimers, respectively. Image size  $150 \text{ \AA} \times 120 \text{ \AA}$ .

of building units of adatom pairs. These adatom pairs, which are also observed as isolated entities (“chains” of length one), are reported to be significantly different from ad-dimers, i.e., stable clusters of two adatoms held together by a lateral bond between the atoms. Similar structures had earlier been observed for Si on Si(100) (Ref. 17) and Si on Ge(100) (Ref. 1) but were not interpreted in terms of a new type of adatom pair. Qin and Lagally suggest in their report that their new interpretation also holds for these systems: “Our own experiments for Si on Si(100) confirm our picture and from a careful analysis of the data we conclude that the same is true for Si on Ge(100) as well.”<sup>10</sup> Here, we show that the latter general statement is not correct: the smallest chainlike structure (two adatoms) for Si on Ge(100) is not the type of adatom pair observed for Ge on Si(100) but can clearly be identified as an ad-dimer. In Fig. 7, a filled-state scanning tunneling microscopy (STM) image of 0.01 monolayer of Si deposited on Ge(001) at room temperature is shown. Two different features, labeled  $D$  and  $I$ , are identified. The epitaxial islands ( $I$ ) consist of dimers positioned alternately at on-top ( $B$ ) and trough ( $D$ ) positions. In accordance with Ge on Si(001), the  $D$  structure [Fig. 1(a) from Ref. 1] appears in a filled-state image as a ringlike feature with a faint intensity in the middle [Fig. 8(a)]. However, in contrast to the observations for Ge on Si(001) by Qin and Lagally,<sup>10</sup> our  $D$  structure is elongated along the substrate dimer-row direction in the empty-state image [Fig. 8(b)] ruling out the possibility of a two-atom unit positioned in neighboring  $M$  sites. Five of

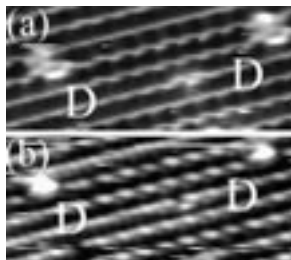


FIG. 8. (a) and (b) High-resolution filled- ( $-1.6$  V) and empty- ( $+1.6$  V) state scanning tunneling microscopy image of a  $D$  structure obtained with a tunneling current of 0.4 nA. Image size  $35 \text{ \AA} \times 100 \text{ \AA}$ .

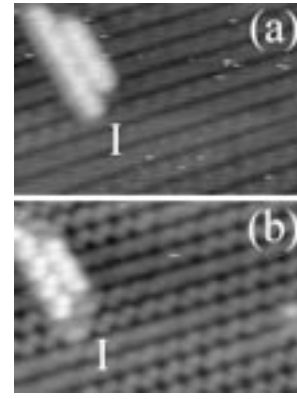


FIG. 9. (a) and (b) High-resolution empty- ( $+1.6$  V) and filled- ( $-1.6$  V) state scanning tunneling microscopy image of an epitaxial island obtained with a tunneling current of 0.4 nA. Image size  $70 \text{ \AA} \times 100 \text{ \AA}$ .

the six end positions of the epitaxial islands ( $I$ ) in Fig. 7 resemble the  $D$  structures (the most left epitaxial island in Fig. 7 terminates at the bottom side with a  $B$  dimer instead of a  $D$  dimer). This is further substantiated by the empty- and filled-state images of an epitaxial island (Fig. 9). The two end dimers of the right side of the epitaxial island in Fig. 9 are visible in the empty-state image, whereas they are nearly invisible in the filled-state image. Therefore, we must conclude that the  $D$  structure consists of an ordinary dimer positioned in the trough with its dimer bond aligned along the substrate dimer-row direction ( $D$  dimer). This is also in accordance with the high thermal stability of the  $D$  structures. Further support in favor of this identification comes from various diffusion events that we have observed at room temperature. We have observed that occasionally dimers located at an on-top position hop to a trough position and vice versa<sup>1</sup> (see Fig. 10).

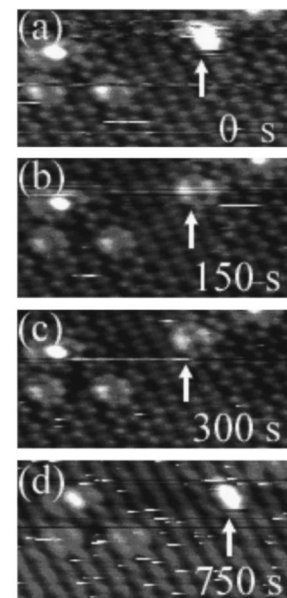


FIG. 10. Four subsequent filled-state STM images. A Si  $A/B$  ad-dimer residing on top jumps to a trough position (a) and (b). In images (c) and (d) it jumps back to an on-top position. Sample bias  $-1.6$  V and tunneling current 0.4 nA. Image size  $160 \text{ \AA} \times 80 \text{ \AA}$ .

In Fig. 10 a sequence of STM images of the same area of the Ge(001) substrate after deposition of  $\approx 0.01$  monolayer Si is shown. In Figs. 10(a)–10(d), the diffusion of a dimer situated on top of a substrate dimer row [Fig. 10(a)] to a trough position [Fig. 10(b)] is shown. In Figs. 10(c) and 10(d), the dimer in the trough position jumps back to an on-top position. Two of these diffusion events may lead to slow diffusion in a direction perpendicular to the substrate dimer rows. The frequency of this event where a dimer hops from an on-top position to a trough position at room temperature is  $\approx 10^{-4}$  hops per second, which translates into an activation barrier of about 1 eV assuming an attempt factor of  $10^{13}$  Hz. Using dual bias imaging we have identified the various adsorption sites for Si ad-dimers on Ge(001). The energetically most stable adsorption site for a Si ad-dimer is in the trough between the substrate dimer-rows with the dimer bond of the ad-dimer aligned along the substrate dimer-row direction. At room temperature, Si ad-dimers occasionally jump from a position on top of the substrate dimer row to a trough position or vice versa. The activation barrier

for the former process is 1 eV assuming an attempt frequency of  $10^{13}$  Hz, whereas the activation barrier for the latter process is slightly higher. Si ad-dimers residing on top of substrate dimer rows at room temperature exhibit a rotational mode between two configurations where the dimer bond is aligned along and parallel to the substrate dimer bond direction, respectively. The rate limiting activation barrier for this process is estimated to be 0.7 eV assuming a preexponential of  $10^{13}$  Hz. The preferential diffusion direction for Si ad-dimers residing on top of the substrate dimer rows is parallel to the dimer rows. The diffusion barrier is  $0.83 \pm 0.05$  eV (assuming an attempt frequency of  $10^{13 \pm 1}$  Hz).

H.J.W.Z and E.Z. acknowledge support from the Netherlands Organization for Scientific Research (NWO) and G.R. acknowledges support by the Deutsche Forschungsgemeinschaft (DFG) and by the Dutch Foundation for Fundamental Research on Matter (FOM).

<sup>1</sup>W. Wulfhekel, B. J. Hattink, H. J. W. Zandvliet, G. Rosenfeld, and B. Poelsema, Phys. Rev. Lett. **79**, 2494 (1997).

<sup>2</sup>R. E. Honig, J. Chem. Phys. **22**, 1610 (1954).

<sup>3</sup>R. A. Wolkow, Phys. Rev. Lett. **74**, 4448 (1995).

<sup>4</sup>D. Dijkkamp, E. J. van Loenen, and H. B. Elswijk, in *Ordering at Surfaces and Interfaces*, edited by A. Yoshimori, T. Shinjo, and H. Watanabe (Springer, Berlin, 1992), p. 85.

<sup>5</sup>Z. Zhang, F. Wu, H. J. W. Zandvliet, B. Poelsema, H. Metiu, and M. G. Lagally, Phys. Rev. Lett. **74**, 3644 (1995).

<sup>6</sup>B. S. Swartzentruber, Phys. Rev. Lett. **76**, 459 (1996).

<sup>7</sup>B. S. Swartzentruber, A. P. Smith, and H. Jónsson, Phys. Rev. Lett. **77**, 2518 (1996).

<sup>8</sup>B. Borovsky, M. Krueger, and E. Ganz, Phys. Rev. Lett. **78**, 4229 (1997).

<sup>9</sup>M. Krueger, B. Borovsky, and E. Ganz, Surf. Sci. **385**, 146 (1997).

<sup>10</sup>X. R. Qin and M. G. Lagally, Science **278**, 1444 (1997).

<sup>11</sup>G. Brocks, P. J. Kelly, and R. Car, Surf. Sci. **269/270**, 860 (1992).

<sup>12</sup>P. J. Bedrossian, Phys. Rev. Lett. **74**, 3648 (1995).

<sup>13</sup>T. Yamasaki, T. Uda, and K. Terakura, Phys. Rev. Lett. **76**, 2949 (1996).

<sup>14</sup>C. M. Goringe and D. R. Bowler, Phys. Rev. B **56**, R7073 (1997).

<sup>15</sup>G. Ehrlich, J. Chem. Phys. **44**, 1050 (1996).

<sup>16</sup>Error weighted linear regression of the data shown in Fig. 6 yields a value of  $\nu = 0.088 \pm 0.002 \text{ s}^{-1}$ . Given the fact that according to Eq. (2) this possibly underestimates the true value of  $\nu$  by about 15%, we give as our best estimate  $\nu = 0.10 \pm 0.01 \text{ s}^{-1}$ .

<sup>17</sup>J. van Wingerden, A. van Dam, M. J. Haye, P. M. L. O. Scholte, and F. Tuinstra, Phys. Rev. B **55**, 4723 (1997).